

A homozygous missense variant in laminin subunit beta 1 as candidate causal mutation of hemifacial microsomia in Romagnola cattle

Joana G. P. Jacinto^{1,2}  | Irene M. Häfliger² | Marco Bernardini^{3,4}  |
Maria Teresa Mandara⁵  | Ezio Bianchi⁶ | Marilena Bolcato¹  |
Noemi Romagnoli¹ | Arcangelo Gentile¹  | Cord Drögemüller² 

¹Department of Veterinary Medical Sciences, University of Bologna, Ozzano, Italy

²Institute of Genetics, Vetsuisse Faculty, University of Bern, Bern, Switzerland

³Anicura Portoni Rossi Veterinary Hospital, Zola Predosa, Bologna, Italy

⁴Department of Animal Medicine, Productions and Health, University of Padua, Padua, Italy

⁵Department of Veterinary Medicine, Neuropathology Laboratory, University of Perugia, Perugia, Italy

⁶Department of Veterinary Medical Sciences, University of Parma, Parma, Italy

Correspondence

Joana G. P. Jacinto, Department of Veterinary Medical Sciences, University of Bologna, Ozzano, Italy.

Email: joana.goncalves2@studio.unibo.it

Abstract

Hemifacial microsomia (HFM) was diagnosed in a 9-day-old Romagnola calf. The condition was characterized by microtia of the left ear, anotia of the right ear, asymmetry of the face, and deafness. Magnetic resonance imaging revealed agenesis of the right pinna and both tympanic bullae, asymmetry of the temporal bones and temporomandibular joints, and right pontine meningocele. Brainstem auditory evoked responses confirmed the impaired auditory capacity. At gross post mortem examination, there was agenesis and hypoplasia of the right and the left external ear, respectively. No histological abnormalities were detected in the inner ears. A trio whole-genome sequencing approach was carried out and identified a private homozygous missense variant in *LAMB1* affecting a conserved residue (p.Arg668Cys). Genotyping of 221 Romagnola bulls revealed a carrier prevalence <2%. This represents a report of a *LAMB1*-related autosomal recessive inherited disorder in domestic animals and adds *LAMB1* to the candidate genes for HFM.

KEYWORDS

Bos taurus, development, microtia, precision medicine, rare disease, WGS

1 | INTRODUCTION

Microtia is a congenital malformation of the external ear and can range in severity from mild structural abnormalities to complete absence of the ear (anotia).¹ It occurs as an isolated malformation (nonsyndromic form) or as a part of a spectrum of anomalies

(syndromic form). Hemifacial microsomia (HFM) is the term used to describe a syndromic form that might be characterized by microtia, facial asymmetry, oral clefts, and eyelid defects. Renal abnormalities, cardiac defects, polydactyly, and vertebral deformities are ancillary malformations.^{2,3}

The causes of microtia are poorly understood in both humans and animals,⁴ although evidence supports contribution of genetic and environmental components. In humans, there are several monogenic inherited mostly syndromic forms of microtia (OMIM 600674 occur associated with disease-causing variants in genes such as *HOXA1*,⁵

Abbreviations: BAs, brachial arches; BAERs, brainstem auditory evoked responses; CNCCs, cranial neural crest cells; H&E, hematoxylin and eosin; HFM, hemifacial microsomia; IGV, Integrative Genomics Viewer; MRI, magnetic resonance imaging; NCCs, neural crest cells; NHL, normal hearing level; WGS, whole-genome sequencing; EGF, epidermal growth factor.

This is an open access article under the terms of the Creative Commons Attribution-NonCommercial-NoDerivs License, which permits use and distribution in any medium, provided the original work is properly cited, the use is non-commercial and no modifications or adaptations are made.

© 2021 The Authors. *Journal of Veterinary Internal Medicine* published by Wiley Periodicals LLC on behalf of American College of Veterinary Internal Medicine.

HOXA2,^{6,7} *ORC1*, *ORC6*, *CDT1*,⁸ *ORC4*,⁹ *CDC6*,¹⁰ *MCM5*,¹¹ *TCOF1*,¹² *POLR1C*, *POLR1D*,¹³ *POLR1B*,¹⁴ and *FGF3*.¹⁵ Mouse model studies identify a list of genes associated with microtia, and illustrated several signaling pathways, including BMP, WNT, FGF, and retinoic acid, that present an important function in outer-ear development.² Furthermore, in cattle and sheep dominantly inherited nonsyndromic forms of anomalies affecting the outer ear are associated with regulatory variants affecting the expression of *HMX1*^{16,17} (OMIA 000317-9913 and OMIA 001952-9940). A recessive syndromic form of microtia in pigs is associated with a deletion in *HOXA1*⁴ (OMIA 001952-9823).

The aims of this study were to describe the clinical and disease phenotype observed in a Romagnola calf affected by HFM, to identify the suspected genetic etiology by a trio-based whole-genome

sequencing (WGS) approach, and to estimate the prevalence of the deleterious allele in Romagnola cattle.

2 | CASE DESCRIPTION

A 9-day-old female Romagnola calf, weighting 43 kg, was admitted to the Department of Veterinary Medical Sciences, University of Bologna because absence of the auricles and facial asymmetry.

At the time of admission, the calf had asymmetry of the face with deviation to the right side and lingual ptosis (Figure 1A). The right pinna was absent (anotia), while the left 1 was a rudiment of soft tissue with absence of the ear canal (aural atresia) and covered by long

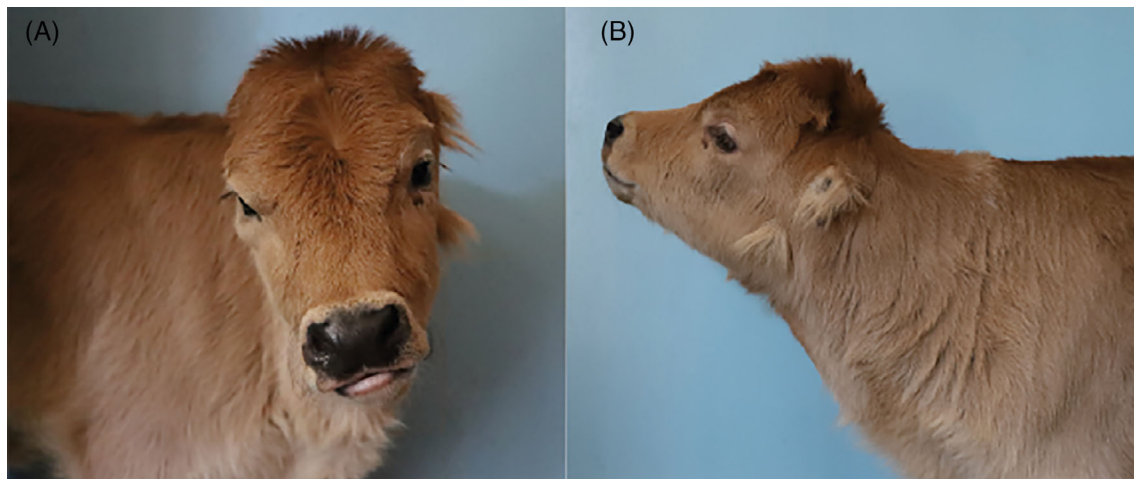


FIGURE 1 Hemifacial microsomia (HFM) in the Romagnola calf demonstrating: (A) note the abnormal conformation of the splanchnocranium with slight right deviation from the sagittal plan and (B) note that the left pinna is a rudiment of soft tissue with absence of the ear canal (aural atresia) and covered by long hair

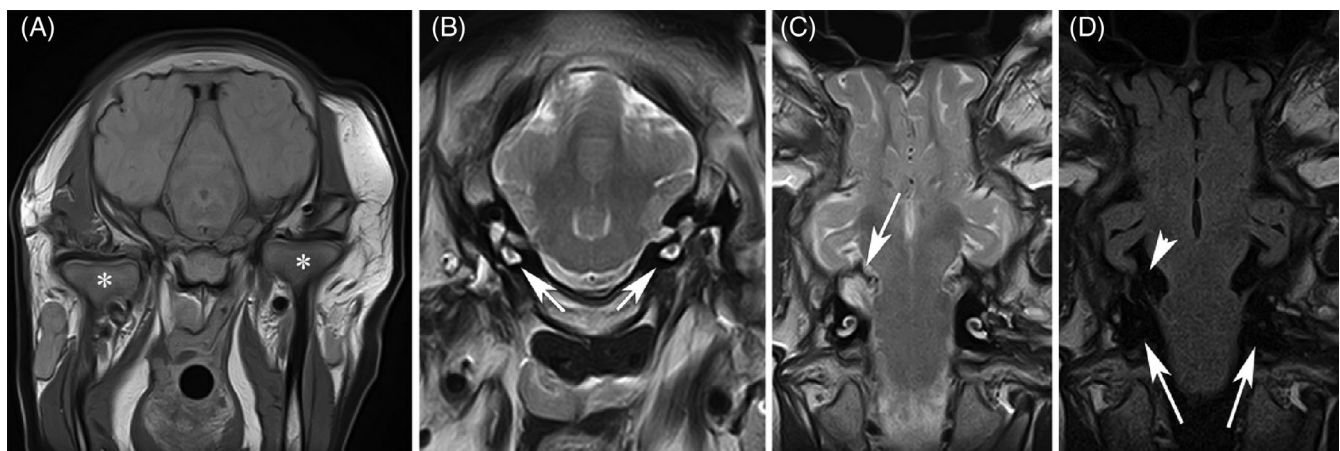


FIGURE 2 Magnetic resonance imaging of the head in the Romagnola calf with hemifacial microsomia (HFM). (A) Transverse proton density image at the level of the caudal mesencephalon. There is marked asymmetry of the temporomandibular joints (asterisks) and the surrounding soft tissues. (B) Transverse T2-weighted image at the level of the pons. There is a normal hyperintense signal of the perilymph and endolymph in both inner ears (arrows). Note the bilateral agenesis of the tympanic bullae. (C) Dorsal T2-weighted image at the level of the inner ears. An enlargement of the subarachnoidal space (meningocele) is seen on the right side at the level of the pons (arrow). (D) Dorsal fluid-attenuated inversion recovery (FLAIR) image at the same level as (C). The T2-weighted hyperintense signal from the inner ears (long arrows) and cerebrospinal fluid in the meningocele (arrow head) is suppressed

hair (Figure 1B). The neurological examination revealed reduced mental status characterized by decreased level of consciousness with listlessness and drowsiness. Notably, the calf did not respond to loud noises and hand clapping. It had a normal stance and gait. A deficit of proprioception was detected in the forelimbs.

Hematology revealed lymphocytosis ($6030/\text{mm}^3$; reference interval, $4250\text{--}5850/\text{mm}^3$) with monocytosis ($1430/\text{mm}^3$) and neutrophilia ($6490/\text{mm}^3$; reference interval, $290\text{--}950/\text{mm}^3$), and hypoproteinemia (5.68 g/dL ; reference interval, $6.74\text{--}7.46\text{ g/dL}$) with hypoalbuminemia (2.79 g/dL ; reference interval, $3.03\text{--}3.55\text{ g/dL}$). Blood samples were tested for bovine viral diarrhea virus, Schmallenberg virus, bluetongue virus, *Neospora caninum*, and *Toxoplasma gondii* using PCR and ELISA for detecting antigens and antibodies, respectively. Tests were negative for all these pathogens using both PCR and ELISA.

The calf underwent general anesthesia for magnetic resonance imaging (MRI) of the head. Magnetic resonance imaging was obtained using a 1.5 T scanner. T2-weighted images were acquired in transverse, sagittal, and dorsal planes, T1-weighted images were acquired in the transverse plane, fluid attenuated inversion recovery (T2-FLAIR) images were acquired in the dorsal plane, and proton density images were acquired in the transverse plane. Slice thickness was 3 to 4 mm, with a 10% interslice gap. Field of view was 16 to 18 cm. No contrast medium was administered. Magnetic resonance imaging revealed: asymmetry of the temporal bones and the temporomandibular joints associated with a right pontine meningocele (Figure 2A,C,D); agenesis of the right external ear canal and both tympanic bullae (Figure 2B). Moreover, on the left side, a structure resembling the innermost part of the external ear canal in shape and location was detected. There was no cavitation. T2-weighted images showed bilaterally a normally shaped, hyperintense signal of the endolymphatic and perilymphatic fluids contained in the inner ear.

Brainstem auditory evoked responses (BAERs) were examined. The signal was amplified 200 000 times, filtered with a bandwidth of 160 to 2000 Hz, and averaged 500 times. Automatic artifact rejection was used with an analysis time of 10 ms. The recording montage was vertex (noninverting input of the amplifier) and ipsilateral mastoid (inverting input). Ground electrode was inserted at the base of the neck. Recording and ground electrodes were stainless steel needles. Acoustic and bone stimuli, produced by electrical square waves of 0.1 ms with a delivery rate of 10/s, were used. Acoustic stimuli were alternating clicks of 95 dB normal hearing level (NHL) delivered monaurally using an audiometric earphone. Bone stimulation was performed with a specific transducer applied to the ipsilateral mastoid bone at a stimulus intensity of 95 dB NHL. For each ear and type of stimulation, 2 tracings were obtained and superimposed to show reproducibility of the responses. The BAERs confirmed the impaired auditory capacity with no evidence of acoustic or bone stimulation at high intensities in ear.

Three months after hospitalization the calf was euthanized because of a severe pneumonia not apparently related to the primary disease.

The calf was subsequently submitted for necropsy. Macroscopically, the left pinna was hypoplastic and the opening of the external

ear canal closed by haircoat while the right pinna was absent and no anatomical remains were found. After decalcification on formalin fixed tissue, macroscopic examination was performed on cut surface having cochlea and semicircular canals aligned. On transversal cut surface, it was completely occupied by chondroid tissue. No abnormalities were detected in the inner ears and brain. Due to the absence of cerebrospinal fluid pressure after detachment of the head, the pontine meningocele observed on the right side by MRI was not detected. Additional findings were severe bronchopneumonia, complete ectopia of the spiral loop of the ascending colon, and numerous nonperforated abomasal ulcers.

Both the ear regions and brain were collected for histopathology. They were fixed in 10% neutral buffered formalin and 5 μm paraffin embedded sections were routinely stained with hematoxylin and eosin (H&E). Formalin-fixed paraffin-embedded 5 μm transverse sections of the brain were stained with H&E and Luxol-fast blue-periodic acid-Schiff methods. Histological abnormalities were not observed in both brain tissue and inner ears. The clinical and pathological findings resembled a form of HFM.

Several inbreeding loops between the unaffected parents were found in the pedigree of the calf. In light of this obvious consanguinity, the presented case of bovine HFM was hypothesized to be a rare recessively inherited variant. Therefore, WGS using the Illumina NovaSeq6000 was performed on DNA extracted from EDTA-blood of the HFM-affected calf, its dam, and from semen of its sire. The sequenced reads were mapped to the ARS-UCD1.2¹⁸ reference genome resulting in an average read depth of approximately $18.1\times$ in the calf, $17.9\times$ in the dam, and $19.2\times$ in the sire and subsequently single-nucleotide variants and small indel variants were called. The applied software and steps to process fastq-files into binary alignment map and genomic variant call format files were in accordance with the

TABLE 1 Results of variant filtering of the HFM-affected calf using the whole-genome sequence data of both parents and 4706 control genomes

Filtering step	Homozygous variants	Heterozygous variants
All variants in the affected calf	3 896 484	4 757 749
Private variants in the affected calf	104 207	1423
Private variants in the affected calf with obligatory carrier parents (protein-changing)	99 443 (245)	NA
Protein-changing private variants with obligatory carrier parents (recessive inheritance)	5	NA
Protein-changing private variants absent in both parents (de novo mutations)	NA	0

Abbreviations: HFM, hemifacial microsomia; NA, not applicable.

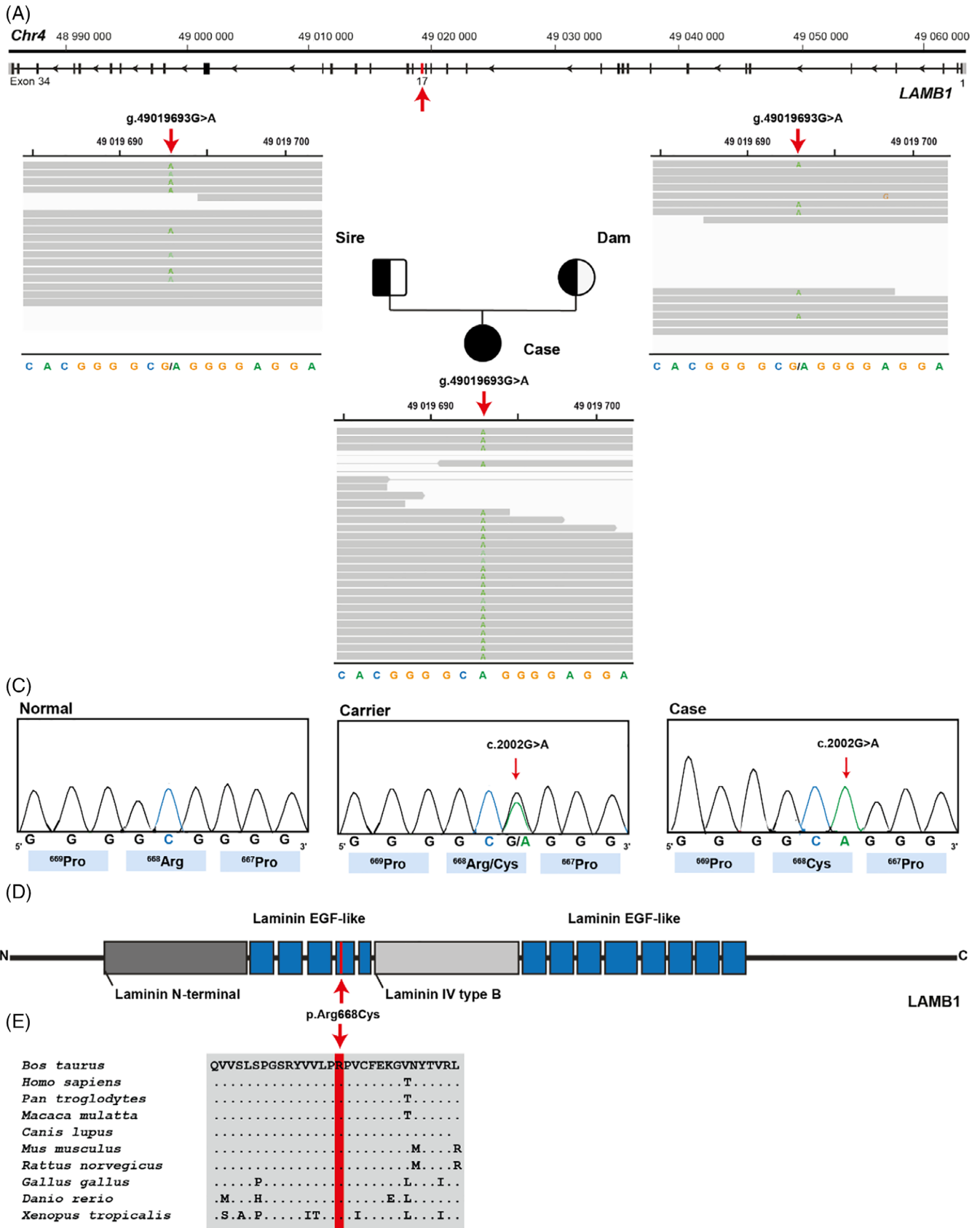


FIGURE 3 Legend on next page.

TABLE 2 Pathogenicity prediction results for the 5 homozygous protein-changing variants exclusively present in the genome of the affected calf and absent in the global control cohort of more than 4700 genomes of a variety of breeds

Gene	OMIM	Associated disorder/gene function	Protein change	Predicted effect	Provean impact and score
<i>LAMB1</i>	150240	Lissencephaly 5	p.Arg668Cys	Deleterious	-4.544
<i>PDCD7</i>	608138	Ceramide-mediated signaling	p.Pro28Leu	Neutral	-1.677
<i>CLMN</i>	611121	Specifically expressed at the final stage of spermatogenesis	p.Lys988Arg	Neutral	-0.310
<i>MEX3C</i>	611005	Phosphoproteins that bound RNA	p.Ala12Pro	Neutral	-0.087
<i>DCC</i>	120470	Colorectal cancer; esophageal carcinoma; Gaze palsy, familial horizontal, with progressive scoliosis, 2	p.Cys36Arg	Neutral	1.322

TABLE 3 Association of the p.Arg668Cys missense variant in *LAMB1* with the hemifacial macrosomia (HFM) phenotype in Romagnola cattle

	Genotype (R = Arg; C = Cys)		
	RR	RC	CC
HFM affected calf	0	0	1
Obligate carriers ^a	NA	2	0
Normal Romagnola control bulls	216	5	0
Normal control cattle from various breeds	4706	0	0

Abbreviation: NA, not applicable.

^aParents of the affected animal.

1000 Bull Genomes Project processing guidelines of run 7 (www.1000bullgenomes.com),¹⁹ except for the trimming, which was performed using fastp.²⁰ Further preparation of the genomic data was done as reported earlier.²¹ In order to find private variants, the genotype of the affected calf was compared with 4706 controls, including 596 cattle genomes of various breeds that had been sequenced in the course of other ongoing studies at the Institute of Genetics of the University of Bern (Table S1) as well as 4110 genomes of a variety of breeds included in run 8 of the 1000 Bull Genomes Project.¹⁸ The generated sequence data are publicly available in the European Nucleotide Archive (SAMEA7015114 is the sample accession number of the affected calf; SAMEA7690202 is the sample accession number of the dam and SAMEA7690203 of the sire; <http://www.ebi.ac.uk/en>).

Integrative Genomics Viewer (IGV)²² software version 2.0 was used for visual inspection of genome regions containing candidate variants. Assuming recessive inheritance in a trio-based approach, filtering of WGS data for homozygous coding variants present in the calf and heterozygous in the parental genomes identified 99 443 variants of which 245 were protein-changing with a predicted high or moderate impact (Table 1). These 245 variants were further investigated for their occurrence in a global control cohort of 4706 genomes of a variety of breeds, which revealed 5 remaining protein-changing variants that were exclusively homozygous in the genome of the affected calf and heterozygous in its parents (Tables 1 and S2).

Among these 5 remaining private variants, 1 single variant affects an interesting candidate gene for the observed phenotype (Figure 3A; Table 2). This homozygous variant at chr4:49019693G>A represents a missense variant in *LAMB1* (NM_001206519.1: c.2002C>T; Figure 3B,C). It alters the encoded amino acid of *LAMB1* residue 668 (NP_001193448.1:p.Arg668Cys) located in the laminin epidermal growth factor (EGF)-like 4 domain (Figure 3D). Furthermore, the arginine to cysteine substitution affects an evolutionary conserved amino acid (Figure 3E) and was predicted to be deleterious²³ (Table 2). To confirm and evaluate the presence of the *LAMB1* variant, the affected genomic region was amplified by PCR and Sanger sequenced in the calf, its dam and sire. Additionally, DNA was extracted from EDTA-blood of 221 Romagnola bulls and genotyping of the *LAMB1* variant was performed. The *LAMB1* missense variant was genotyped using the following primers: 5'- GTAGATGCACGTTGTCTGCC -3' (forward primer) and 5'- AGCCAAAACCAGACAGACTA -3' (reverse primer). Analyzing the sequencing data, it was confirmed that the calf was

FIGURE 3 A homozygous *LAMB1* missense variant in the HFM-affected Romagnola calf. (A) *LAMB1* gene structure showing the variant location on chromosome 4, exon 17 (red arrow). References to the bovine *LAMB1* gene correspond to the NCBI accessions NC_037331.1 (chromosome 4, ARS-UCD1.2), NM_001206519.1 (bovine *LAMB1* mRNA). (B) IGV screenshot presenting the Chr4: g. 49019693G>A variant homozygous in the affected calf (shown below) and heterozygous in both parents (top left: sire; top right: dam) revealed by whole-genome sequencing. (C) Electropherograms showing the normal, carrier, and case genotypes obtained by Sanger sequencing. (D) Schematic representation of the bovine *LAMB1* protein and its functional domains obtained from the UniProt database (<http://www.uniprot.org/>; accession number: A0A3S5ZPX3). Laminin N-terminal domain is represented in dark gray; laminin epidermal growth factor (EGF)-like domains are represented in blue; laminin IV type B domain is represented in light gray. (E) Multiple sequence alignment of the laminin EGF-like of *LAMB1* protein encompassing the region of the p.Arg668Cys variant demonstrates complete evolutionary conservation across species. Protein sequences accession numbers in NCBI for each species are NP_001193448.1 (*Bos taurus*), NP_002282.2 (*Homo sapiens*), XP_001165667.2 (*Pan troglodytes*), XP_001090393.2 (*Macaca mulatta*), XP_533089.4 (*Canis lupus*), NP_032508.2 (*Mus musculus*), XP_003750185.1 (*Rattus norvegicus*), XP_415943.3 (*Gallus gallus*), XP_002933140.2 (*Xenopus tropicalis*), NP_775382.1 (*Danio rerio*). HFM, hemifacial macrosomia; IGV, Integrative Genomics Viewer

homozygous and the sire and dam heterozygous for the detected *LAMB1* variant. Furthermore, the genotyping of the 221 Romagnola bulls revealed no homozygous mutant animal and a total of 5 heterozygous carriers (1.13%; Table 3).

Variant filtering revealed no private heterozygous protein-changing variants present in the genome of the HFM-affected calf and absent in both parental genomes and in 4706 controls.

3 | DISCUSSION

In this study, a comprehensive clinical, pathologic, and genetic investigation of a deaf Romagnola calf displaying a form of congenital microtia associated with craniofacial anomalies revealed a putative genetic cause for the abnormality. In humans, 50% of microtia cases are associated with ancillary findings, mostly craniofacial anomalies.^{24,25} Hemifacial microsomia is 1 of the major microtia-related diagnoses in human medicine with an incidence of 1:5600 live births²⁶ and is estimated as the most common birth defect of the human face, after cleft lip and cleft palate. Features of HFM include unilaterally as well as bilaterally deformity of the external ear and small ipsilateral half of the face with epibulbar dermoid and vertebral anomalies (OMIM 164210), leading to asymmetrical appearance.²⁷ Due to a marked phenotypic diversification, no typical clinical picture can be assigned to HFM: it might present from minor asymmetry with deformed auricle or microtia, until complete anotia, with conductive type hearing loss.²⁴

A genetic origin was evaluated assuming either a recessively inherited mutation or alternatively the hypothesis of a dominant acting *de novo* mutation (which occurred in a single parental gamete or happened during early embryonic development of the calf) as the possible cause for this novel congenital phenotype. The trio-based WGS approach identified 5 homozygous and no heterozygous protein-changing variants exclusively present in the genome of the affected calf and absent in a global control cohort. Consequently, a *de novo* mutation as a possible cause for the observed phenotype seems unlikely. After *in silico* effect predictions just the homozygous variant affecting the fourth laminin EGF-like domain of *LAMB1* was predicted to be deleterious. Moreover, within a representative control cohort of the current Italian Romagnola population, a very low allele frequency and the absence of the homozygous genotype for the deleterious allele was noticed. Considering the rarity of this coding variant, the *in silico* effect prediction and the known function of *LAMB1* gene, the identified variant was considered to represent the most likely genetic cause for the observed phenotype. Furthermore, it might be assumed that this pathogenic variant affecting a functional candidate gene is the most plausible explanation.

The candidate gene *LAMB1* encodes laminin subunit beta 1 belonging to laminins that are large molecular weight glycoproteins found in the basal lamina, playing an important role in cell proliferation, differentiation, migration, and adhesion.²⁸ They are cross-shaped heterotrimeric proteins constituted by the assembly of 3 disulfide-linked polypeptides, the α , β , and γ chains from the *LAMA*, *LAMB*, and *LAMC* families, respectively.²⁹ Each individual laminin subunit demonstrates a

specific spatial and temporal expression pattern.³⁰ In mammals, there are at least 15 laminins, and *LAMB1* is present in 6 of them.³¹ Moreover, *LAMB1* is 1 of the earliest laminin subunits expressed during embryogenesis at several sites, including neuroectoderm.^{29,32} The calf in this study had several malformations deriving from neuroectoderm such as the pontine meningocele and malformations of the auricle, middle ear, and temporomandibular region. Hemifacial microsomia affects most structures of the craniofacial region that derive from the first and second brachial arches (BAs). Arising from the neuroectoderm, neural crest cells (NCCs) follow stereotypical migratory pathways and populate the BAs, and cranial NCCs (CNCCs) form the first and second BAs, which contribute to most craniofacial skeleton and connective tissues.³³ Cranial neural crest cells in the first BA form the maxilla, zygomatic bone, mandible, malleus, incus, and trigeminal nerve, which might be affected in HFM. Cranial neural crest cells of the second BA form the stapes and facial nerve.³⁴ Therefore the described phenotype displayed by the calf in this study, including microtia of the left ear and anotia of the right ear, absence of tympanic bullae, deafness and asymmetry of the temporal bones and the temporomandibular joints, strongly resembles human HFM. In veterinary medicine, so far, rare forms of HFM are reported only in cats.³⁵

Mutations in the *LAMB1* gene have been identified and studied at a molecular level in humans (OMIM 150240) and mice (MGI 96743). Pathogenic variants affecting the human *LAMB1* are associated with autosomal recessive diseases such as: cobblestone brain malformation with congenital hydrocephalus, severe developmental delay, and an increased head circumference³⁶; progressive leukoencephalopathy with seizures, ocular abnormalities, and porencephalic lesions³⁷; childhood-onset epilepsy, macrocephaly, and intellectual development arrest³⁸; and adult-onset leukoencephalopathy.³⁹ In mice, heterozygous dominant acting variants in *lamb1* are associated with dystonia-like movement disorder with brain and spinal neuronal defects,⁴⁰ while recessively inherited pathogenic variants are related with embryonic lethality between implantation and somite formation.⁴¹ The calf presented in this study had malformation of the skull; however, no signs of leukoencephalopathy, cobblestone brain malformation, or dystonia were noticed.

This is a report of a pathogenic *LAMB1* variant in domestic animals and of the *LAMB1*-related recessively inherited form of HFM. Therefore, it represents an animal model for the understanding of similar human conditions and adds *LAMB1* to the list of candidate genes for HFM. Humans show developmental, anatomical, and physiological features of the auditory system that are more similar with cattle than with mice. Among these, the fact that compared to mice, cattle and humans can hear at birth. The cattle model thus fits better than the mouse model for understanding human hearing diseases.

In conclusion, this study provides a DNA-based diagnostic test that enables selection against the identified pathogenic variant in Romagnola cattle.

ACKNOWLEDGMENT

No funding was received for this study. The authors acknowledge the Interfaculty Bioinformatics Unit of the University of Bern for providing computational infrastructure. The WGS data are available under

the study accession no. PRJEB18113 at the European Nucleotide Archive (www.ebi.ac.uk/ena; sample accessions SAMEA7015114 [affected calf], SAMEA7690202 [dam], and SAMEA7690203 [sire]). We thank Nathalie Besuchet-Schmutz for expert technical assistance.

CONFLICT OF INTEREST DECLARATION

Authors declare no conflicts of interest.

OFF-LABEL ANTIMICROBIAL DECLARATION

Authors declare no off-label use of antimicrobials.

INSTITUTIONAL ANIMAL CARE AND USE COMMITTEE (IACUC) OR OTHER APPROVAL DECLARATION

Authors declare no IACUC or other approval was needed.

HUMAN ETHICS APPROVAL DECLARATION

Authors declare human ethics approval was not needed for this study.

ORCID

Joana G. P. Jacinto  <https://orcid.org/0000-0002-6438-7975>

Marco Bernardini  <https://orcid.org/0000-0002-8572-0271>

Maria Teresa Mandara  <https://orcid.org/0000-0003-1501-6163>

Marilena Bolcato  <https://orcid.org/0000-0002-0605-3344>

Arcangelo Gentile  <https://orcid.org/0000-0002-6091-8978>

Cord Drögemüller  <https://orcid.org/0000-0001-9773-522X>

REFERENCES

- Suutarla S, Rautio J, Ritvanen A, Ala-Mello S, Jero J, Klockars T. Microtia in Finland: comparison of characteristics in different populations. *Int J Pediatr Otorhinolaryngol.* 2007;71(8):1211-1217.
- Luquetti DV, Heike CL, Hing AV, Cunningham ML, Cox TC. Microtia: epidemiology and genetics. *Am J Med Genet A.* 2012;158A(1):124-139.
- Mastroiacovo P, Corchia C, Botto LD, Lanni R, Zampino G, Fusco D. Epidemiology and genetics of microtia-anotia: a registry based study on over one million births. *J Med Genet.* 1995;32(6):453-457.
- Qiao R, He Y, Pan B, et al. Understanding the molecular mechanisms of human microtia via a pig model of HOXA1 syndrome. *Dis Model Mech.* 2015;8(6):611-622.
- Tischfield MA, Bosley TM, Salih MAM, et al. Homozygous HOXA1 mutations disrupt human brainstem, inner ear, cardiovascular and cognitive development. *Nat Genet.* 2005;37(10):1035-1037.
- Alasti F, Sadeghi A, Sanati MH, et al. A mutation in HOXA2 is responsible for autosomal-recessive microtia in an Iranian family. *Am J Hum Genet.* 2008;82(4):982-991.
- Brown KK, Viana LM, Helwig CC, et al. HOXA2 haploinsufficiency in dominant bilateral microtia and hearing loss. *Hum Mutat.* 2013;34(10):1347-1351.
- Bicknell LS, Bongers EMHF, Leitch A, et al. Mutations in the pre-replication complex cause Meier-Gorlin syndrome. *Nat Genet.* 2011;43(4):356-360.
- Guernsey DL, Matsuoka M, Jiang H, et al. Mutations in origin recognition complex gene ORC4 cause Meier-Gorlin syndrome. *Nat Genet.* 2011;43(4):360-365.
- Fenwick AL, Kliszczak M, Cooper F, et al. Mutations in CDC45, encoding an essential component of the pre-initiation complex, cause Meier-Gorlin syndrome and craniosynostosis. *Am J Hum Genet.* 2016;99(1):125-138.
- Vetro A, Savasta S, Russo Raucci A, et al. MCM5: a new actor in the link between DNA replication and Meier-Gorlin syndrome. *Eur J Hum Genet.* 2017;25(5):646-650.
- Edwards SJ, Gladwin AJ, Dixon MJ. The mutational spectrum in Treacher Collins syndrome reveals a predominance of mutations that create a premature-termination codon. *Am J Hum Genet.* 1997;60(3):515-524.
- Schaefer E, Collet C, Genevieve D, et al. Autosomal recessive POLR1D mutation with decrease of TCOF1 mRNA is responsible for Treacher Collins syndrome. *Genet Med.* 2014;16(9):720-724.
- Sanchez E, Laplace-Builhé B, Mau-Them FT, et al. POLR1B and neural crest cell anomalies in Treacher Collins syndrome type 4. *Genet Med.* 2020;22(3):547-556.
- Tekin M, Öztürkmen Akay H, Fitoz S, et al. Homozygous FGF3 mutations result in congenital deafness with inner ear agenesis, microtia, and microdontia. *Clin Genet.* 2008;73(6):554-565.
- He S, Zhang Z, Sun Y, et al. Genome-wide association study shows that microtia in Altay sheep is caused by a 76 bp duplication of HMX1. *Anim Genet.* 2020;51(1):132-136.
- Koch CT, Bruggmann R, Tetens J, Drögemüller C. A non-coding genomic duplication at the HMX1 locus is associated with crop ears in highland cattle. *PLoS One.* 2013;8(10):e77841.
- Rosen BD, Bickhart DM, Schnabel RD, et al. De novo assembly of the cattle reference genome with single-molecule sequencing. *Gigascience.* 2020;9(3):1-9.
- Hayes BJ, Daetwyler HD. 1000 bull genomes project to map simple and complex genetic traits in cattle: applications and outcomes. *Annu Rev Anim Biosci.* 2019;7:89-102.
- Chen S, Zhou Y, Chen Y, Gu J. Fastp: an ultra-fast all-in-one FASTQ preprocessor. *Bioinformatics.* 2018;34(17):i884-i890.
- Häfliger IM, Wiedemar N, Švara T, et al. Identification of small and large genomic candidate variants in bovine pulmonary hypoplasia and anasarca syndrome. *Anim Genet.* 2020;51(3):382-390.
- Robinson JT, Thorvaldsdóttir H, Wenger AM, Zehir A, Mesirov JP. Variant review with the integrative genomics viewer. *Cancer Res.* 2017;77(21):e31-e34.
- Choi Y, Chan AP. PROVEAN web server: a tool to predict the functional effect of amino acid substitutions and indels. *Bioinformatics.* 2015;31(16):2745-2747.
- Paul MA, Opyrczał J, Knakiewicz M, Jaremków P, Bajtek J, Chrapusta A. Hemifacial microsomia review: recent advancements in understanding the disease. *J Craniofac Surg.* 2020;31(8):2123-2127.
- Hartzell LD, Chinnadurai S. Microtia and related facial anomalies. *Clin Perinatol.* 2018;45(4):679-697.
- Wolford LM, Perez DE. Surgical management of congenital deformities with temporomandibular joint malformation. *Oral Maxillofac Surg Clin North Am.* 2015;27(1):137-154.
- Gougoutas AJ, Singh DJ, Low DW, Bartlett SP. Hemifacial microsomia: clinical features and pictographic representations of the OMENS classification system. *Plast Reconstr Surg.* 2007;120(7):112e-113e.
- Lee J, Gross JM. Laminin beta1 and gamma1 containing laminins are essential for basement membrane integrity in the zebrafish eye. *Invest Ophthalmol Vis Sci.* 2007;48(6):2483-2490.
- Roediger M, Miosge N, Gersdorff N. Tissue distribution of the laminin β 1 and β 2 chain during embryonic and fetal human development. *J Mol Histol.* 2010;41(2-3):177-184.
- Sharif KA, Li C, Gudas LJ. cis-acting DNA regulatory elements, including the retinoic acid response element, are required for tissue specific laminin B1 promoter/lacZ expression in transgenic mice. *Mech Dev.* 2001;103(1-2):13-25.
- Sharif KA, Baker H, Gudas LJ. Differential regulation of laminin b1 transgene expression in the neonatal and adult mouse brain. *Neuroscience.* 2004;126(4):967-978.

32. Baldarelli RM, Smith CM, Finger JH, et al. The mouse Gene Expression Database (GXD): 2021 update. *Nucleic Acids Res.* 2021;49(D1):D924-D931.
33. Minoux M, Rijli FM. Molecular mechanisms of cranial neural crest cell migration and patterning in craniofacial development. *Development.* 2010;137(16):2605-2621.
34. Johnson JM, Moonis G, Green GE, Carmody R, Burbank HN. Syndromes of the first and second branchial arches, part 1: embryology and characteristic defects. *AJNR Am J Neuroradiol.* 2011;32(1):14-19.
35. Song RB, Kent M, Glass EN, Davis GJ, Castro FA, de Lahunta A. Hemifacial microsomia in a cat. *Anat Histol Embryol.* 2017;46(5):497-501.
36. Radmanesh F, Caglayan AO, Silhavy JL, et al. Mutations in LAMB1 cause cobblestone brain malformation without muscular or ocular abnormalities. *Am J Hum Genet.* 2013;92(3):468-474.
37. Tonduti D, Dorboz I, Renaldo F, et al. Cystic leukoencephalopathy with cortical dysplasia related to LAMB1 mutations. *Neurology.* 2015;84(21):2195-2197.
38. Okazaki T, Saito Y, Hayashida T, et al. Bilateral cerebellar cysts and cerebral white matter lesions with cortical dysgenesis: expanding the phenotype of LAMB1 gene mutations. *Clin Genet.* 2018;94:391-392.
39. Yasuda R, Yoshida T, Mizuta I, et al. Adult-onset leukoencephalopathy with homozygous LAMB1 missense mutation. *Neurol Genet.* 2020;6(4):4-7.
40. Liu YB, Tewari A, Salameh J, et al. A dystonia-like movement disorder with brain and spinal neuronal defects is caused by mutation of the mouse laminin β 1 subunit, Lamb1. *Elife.* 2015;4:e11102.
41. Miner JH, Li C, Mudd JL, Go G, Sutherland AE. Compositional and structural requirements for laminin and basement membranes during mouse embryo implantation and gastrulation. *Development.* 2004;131(10):2247-2256.

SUPPORTING INFORMATION

Additional supporting information may be found in the online version of the article at the publisher's website.

How to cite this article: Jacinto JGP, Häfliger IM, Bernardini M, et al. A homozygous missense variant in laminin subunit beta 1 as candidate causal mutation of hemifacial microsomia in Romagnola cattle. *J Vet Intern Med.* 2021;1-8. doi:10.1111/jvim.16316